HEDL SA-2101

MASTER

MECHANICAL MODEL FOR DUCTILITY LOSS

W. L. Hu

February 11, 1980

To be presented at the 13th National Symposium on Fracture Mechanics Meeting on June 16-18, 1980 in Philadelphia, PA.

HANFORD ENGINEERING DEVELOPMENT LABORATORY
Operated by Westinghouse Hanford Company, a subsidiary of Westinghouse Electric Corporation, under the Department of Energy Contract No. EY-76-C-14-2170

DISCLAIMER

CONF-800673--2

MECHANICAL MODEL FOR DUCTILITY LOSS

W. L. Hu and G. L. Wire
Hanford Engineering Development Laboratory

ABSTRACT

A mechanical model was constructed to probe into the mechanism of ductility loss. Fracture criterion based on critical localized deformation was undertaken. Two microstructure variables were considered in the model. Namely, the strength ratio of grain boundary affected area to the matrix, Ω, and the linear fraction, x, of grain boundary affected area. A parametrical study was carried out. The study shows that the ductility is very sensitive to those microstructure parameters. The functional dependence of ductility to temperature as well as strain-rate, suggested by the model, is demonstrated to be consistent with the observation.

INTRODUCTION

The high-temperature fracture of austenitic stainless steels and nickel base superalloys is generally identified as intergranular. It has been widely accepted that the grain boundary fracture process is often associated with loss of tensile ductility.[1,2,3] Several models[4,5,6] have been proposed on the contribution of the grain boundary sliding to the intergranular fracture process. Unfortunately, most of the models only treated the micromechanisms involved and, hence, were limited to certain specific materials under specific testing conditions. A correlation between the gross mechanical properties and the microfracture process is yet to be established. This study, based on an extension of Hart's model[7] of intergranular failure, is intended to provide a linkage between the gross mechanical properties and the microstructures. The effects of microstructural characteristics on the ductility and fracture mode, under various strain rates and testing temperatures, are discussed.

EXPERIMENTAL OBSERVATION AND EVIDENCE

Before going into the derivation of the mechanical model, a brief discussion of the experimental observations associated with ductility loss is appropriate. It has been noted that the fracture morphology indicated that ductility loss is normally associated with intergranular failure at elevated temperature.[1,2] If the material behaves in a truly brittle manner, a single crack will lead the specimen to a premature failure. Microstructure investigation revealed,[3] however, that multiple microcracks do form prior to failure, preferably normal to the applied stress, which suggested that failure is not crack-sensitive in the same way that ferritic steels are at low temperature. By this, it is meant that these materials are not subject to cleavage. Other supporting evidence resulted from the fact that fracture strength is close to the yield strength of the material. (The yield strength at elevated temperature, where total ductility loss occurs, is not measured but extrapolated from the data at lower testing temperatures.) Consequently, sizable plastic deformation must take place ahead of any microcracks before

failure. The nature of the microstructural observation, together with the high fracture strength to yield strength ratio, led us to conclude that failure is likely caused by highly localized ductile fracture mechanisms. It is also interesting to note that loss of ductility is strain-rate sensitive and it occurred at temperatures near one-half of the melting point of the material. Both of the above observations are consistent with the characteristic of the grain boundary sliding model proposed by Hart.

MECHANICAL MODEL

Hart showed that if the boundary sliding velocity were related to the tangential stress of the boundary in the Newtonian form

$$\sigma_T = kv \tag{1}$$

and if the matrix flow stress depended on the matrix strain-rate as conventional power law form

$$\sigma = \sigma_o \dot{\varepsilon}_m^{\mu} \tag{2}$$

then, by taking due account of the mechanical interactions of boundary and matrix, it was not difficult to deduce a σ-$\dot{\varepsilon}$ behavior for most of the polycrystalline materials.

The physical picture of the present model is shown on the left side of Figure 1 and the rheological diagram is shown at the right. This model deviates from Hart's original model on two counts. First, in Hart's model, the accommodation of grain boundary sliding is confined in a narrow area adjacent to the grain boundary. A previous investigation[8] showed that based on differences deduced between sliding measured longitudinally and transversely,

that sliding takes place in a zone considerably wider than the actual boundary transition. This is represented by a parameter x which represents the fraction of the grain in the grain boundary affected zone. Considering the small gage length of grain boundary, it is not surprising to see that ductility is a sensitive function of x. Second, within this grain boundary affected zone, the strength of the material is allowed to be different from that of the matrix. The strength ratio of the grain boundary affected zone to the matrix is denoted as Ω. Because failure occurs intergranularly, the grain boundary appears to be the weaker link in the whole system. Therefore, Ω is always taken to be smaller than 1.

The detailed schematic illustration near the triple point is shown in Figure 2. The applied stress, σ, is decomposed into normal and tangential components, σ_N and σ_T, respectively. At the triple point, the tangential component is reduced by an amount equal to kv because of the resistance of Newtonian flow. The triple point now behaves as a pseudo-crack tip subjected to the boundary condition σ_N and σ_T - kv. Following the standard elastic solution of a cracked body[9], the shear stress ahead of the crack tip is of the form

$$\sigma_{xy} = A_1(\alpha,\theta)\,\sigma\sqrt{\frac{d}{2r}} - k\,v\,A_2(\theta)\sqrt{\frac{d}{2r}} \qquad (3)$$

where α is the angle measured from the loading direction to the inclined crack surface, and θ and r are defined in Figure 2. Further, material compatibility requires that sliding velocity be accommodated by the integration of shear strain-rate ahead of sliding boundary,

$$v = \int \dot{\varepsilon}_{xy}\, dy \qquad (4)$$

where the shear strain-rate, $\dot{\varepsilon}_{xy}$, is related to shear stress, σ_{xy}, in an expression like Equation (2) with $\Omega\sigma_o$ substituted for σ_o,

$$\sigma_{xy} = \Omega \sigma_o \dot{\varepsilon}_{xy}^{\mu} \tag{5}$$

In this study, σ_o is the ultimate tensile strength of the material at lower test temperatures where the failure morphology is transganular, and hence it represents the strength of the matrix. Strain-rate sensitivity, μ, is approximately equal to 0.07.[10]

At this point, some understanding of plastic behavior ahead of a crack tip might be helpful for further derivation. Considering an inclined crack in a homogeneous material under the boundary stresses

$$\sigma_N = \sigma \operatorname{Sin}^2 \alpha$$
$$\sigma_T = \sigma \operatorname{Sin}\alpha \operatorname{Cos}\alpha - kv \tag{6}$$

we assume

$$kv = (1 - R)\sigma \operatorname{Sin}\alpha \operatorname{Cos}\alpha \tag{7}$$

in which R, changing from 0 to 1, indicates various degress of shear resistance along the cracked surface. A crude estimation of plastic zone size may be obtained by calculating the effective stress, $\bar{\sigma}$, ahead of the crack tip and identifying the locus of $\bar{\sigma} = \sigma_Y$ as the end of the plastic zone. The locus shape for two values of α is shown in Figure 3 for various R at applied stress equal to $0.8\sigma_Y$. It is demonstrated that the plastic zone size is in the range of 0.1 of the crack length, which means that fracture is accompanied by a significant amount of local deformation. In switching from

the aforementioned homogeneous material behavior to the more realistic composite structure of grain boundary and matrix, it is reasonable, therefore, to assume that all the accommodation be plastic and that it be confined within the grain boundary affected zone. Moreover, recognizing the relatively low work-hardening behavior at elevated temperatures, the shear stress can be assumed to be independent of distance from crack tip and to be only a function of θ and α, i.e.,

$$\sigma_{xy} = \sqrt{\frac{d}{xD}} \left(A_1 \sigma - A_2 k v \right) \tag{8}$$

where d is the length of the sliding boundary, which is directly proportional to the linear dimension of the grain size D. Substituting Equations (5) and (8) into Equation (4) and noting that the grain boundary strain rate, $\dot{\varepsilon}_g$, is identified by v/d, it follows that

$$\dot{\varepsilon}_g = \frac{1}{d} \int \left[\frac{1}{\Omega \sigma_o} \sqrt{\frac{d}{xD}} \left(A_1 \sigma - A_2 k d \dot{\varepsilon}_g \right) \right]^{1/\mu} dy \tag{9}$$

The range of the integration is extended over the grain boundary affected region, xD. Introducing two geometrical factors A and A' as

$$\begin{aligned} A^{1/\mu} xd &= \int \left(\sqrt{d/D}\ A_1 \right)^{1/\mu} dy \\ A'^{1/\mu} xd &= \int \left(\sqrt{d/D}\ A_2 \right)^{1/\mu} dy \end{aligned} \tag{10}$$

Apart from a shape factor, $\sqrt{d/D}$, A, and A' are practically the average value of A_1 and A_2 over the range of integration. For further calculation, A and A' are taken to be 0.1 and 0.2 respectively. Inserting Equation (10) into Equation (9) and rearranging, the applied stress can now be related explicitly

to grain boundary strain-rate as

$$\sigma = \frac{\Omega \sigma_o}{A} X^{0.5-\mu} \dot{\varepsilon}_g^{\mu} + \frac{A'}{A} k d \dot{\varepsilon}_g \tag{11}$$

Equation (2) and Equation (11) give the required stress and strain-rate behavior. It can be further reduced by the following substitutions:

$$\dot{e}_g \equiv \dot{\varepsilon}_g / \dot{\varepsilon}_0 \quad \dot{e}_m \equiv \dot{\varepsilon}_m / \dot{\varepsilon}_0 \quad \dot{e} \equiv \dot{\varepsilon} / \dot{\varepsilon}_0$$

$$S \equiv \sigma / \sigma_0 \dot{\varepsilon}_0^{\mu} \tag{12}$$

$$Y \equiv \frac{\Omega}{A} X^{0.5-\mu}$$

$$\dot{\varepsilon}_0 \equiv \left(\frac{\Omega \sigma_0}{A' k d} X^{0.5-\mu} \right)^{\frac{1}{1-\mu}}$$

The normalized form is

$$S = Y (\dot{e}_g^{\mu} + \dot{e}_g)$$

$$S = \dot{e}_m^{\mu} \tag{13}$$

Although this derivation follows a different path, Equation (13) is identical to the results previously obtain by Hart. The essential difference is that a better understanding of the parameters involved can now be obtained. The intrinsic relationship between the microstructure properties and mechanical parameters may be examined.

The total elongation of the specimen is the sum of the displacement from the grain boundary area and grain matrix. Accordingly, the total strain is

the sum of the strain components from both regions, each weighted by its gage length. The overall stain-rate is then

$$\dot{e} = (1-x)\,\dot{e}_m + x\,\dot{e}_g \qquad (14)$$

FAILURE CRITERION AND DUCTILITY

The commonly accepted ductile fracture criterion is the J-intergral developed by Rice.[11] A critical J value at fracture identifies a critical elastic-plastic stress and strain field ahead of the crack tip. In the case of a tensile test while the load is monotonically increased, problems of plasticity can be treated as problems of nonlinear elasticity. Therefore, the interrelationship between stresses, strains, and J values is uniquely defined. At elevated temperatures, the material exhibits nearly perfect plastic behavior. As a consequence, the stress field ahead of the crack may be treated as constant with applied load. A critial strain for failure is, hence, reasonable. Accordingly, the fracture criterion employed here is critical grain boundary strain. This criterion is also consistent with the critical crack opening displacement that has been widely accepted, especially in other countries.[12]

The choice of a grain boundary strain failure limit is consistent with behavior observed in creep. Intergranular failure is generally observed in creep fracture of most metallic materials at elevated temperatures. It is well known[13] that the following equation describes the relationship between the steady-state creep rate $\dot{\varepsilon}_s$ and the time to fracture t_f:

$$\dot{\varepsilon}_s t_f = \text{Constant} \qquad (15)$$

The proportionality of the creep strain and sliding displacement has been demonstrated elsewhere.[14] If the steady-state creep is the main portion of the whole creep duration up to the fracture, Equation (15) confirms the critical grain boundary strain criterion, i.e.,

$$\varepsilon_{gc} = \text{Constant} \tag{16}$$

where ε_{gc} is the grain boundary strain at fracture.

Total strain to failure is expressed by the following series of self-explanatory equations, where the assumption of no strain hardening is invoked.

$$\varepsilon = \int \dot{\varepsilon}\, dt = \frac{\dot{\varepsilon}}{\dot{\varepsilon}_g} \int \dot{\varepsilon}_g dt = \frac{\dot{e}}{\dot{e}_g} \int \dot{\varepsilon}_g dt = \frac{\dot{e}}{\dot{e}_g}\, \varepsilon_{gc} \tag{17}$$

An immediate deduction of the ductility in this present model is indicated by the ratio of total strain-rate to the grain boundary strain-rate $\dot{e}/\dot{e}_g$. From Equations (13) and (14), it is easy to see that

$$\dot{e}/\dot{e}_g = \left(\frac{1}{X} - 1\right)\left[\frac{\Omega\sqrt{X}}{A}\left(1 + \dot{e}_g^{\,1-\mu}\right)\right]^{1/\mu} + X \tag{18}$$

If the critical grain boundary strain is taken to be 10% and if the minimum measurable total strain is 0.1%, then practically speaking, zero ductility is realized when $\dot{e}/\dot{e}_g$ is smaller than 0.01.

RESULTS AND DISCUSSIONS

The graphical representation of Equations (13) and (14) are shown in Figure 4 for two values of x. It is clear that at low stress and strain-rate, the grain boundary sliding is the controlling mechanism; whereas at high stress and hence high strain-rate, the matrix deformation becomes the major contribution to the total strain-rate. An interesting point in this figure is when $\dot{e}$, $\dot{e}_m$, and $\dot{e}_g$ intersect each other. This relationship can be easily realized by studying Equation (14). It is clear that when the strain-rate is smaller than the particular strain-rate at the intersection point (denoted by $\dot{e}_c$), $\dot{e}/\dot{e}_g$ starts decreasing sharply and, hence, the ductility decreases sharply. The relationship between $\dot{e}_c$, x, and Ω can be derived by combining Equations (15) and (14) and setting $\dot{e} = \dot{e}_m = \dot{e}_g$. It follows that

$$\dot{e}_c = \left(\frac{A}{\Omega} x^{\mu - 0.5} - 1 \right)^{\frac{1}{1-\mu}} \tag{19}$$

and is plotted in Figure 5.

It is also shown in Figure 4 that the stress-strain rate behavior appears sensitive to x. The strain-rate sensitivity is shown in Figure 6, which indicates that ductility will increase with the total strain-rate. The functional dependence is insensitive to the strength ratio Ω. It was previously indicated that $\dot{e}$ is normalized by a temperature compensating parameter $\dot{\varepsilon}_o$ which is defined in Equation (12) as

$$\dot{\varepsilon}_o \equiv \left(\frac{\Omega \sigma_o}{A' k d} x^{0.5 - \mu} \right)^{\frac{1}{1-\mu}} \tag{20}$$

The major temperature dependent variable in Equation (20) is the viscosity, k. Because the sliding process is dependent on diffusion, it is reasonable to assume k changes with temperature in the form as

$$k = K e^{Q/RT} \tag{21}$$

where K is a material constant,
Q is the activation energy of grain boundary sliding, which is closely approached by the activation energy of diffusional creep,
T is the temperature in absolute scale,
R is the gas constant.

For a nickel base superalloy, Q may be taken to be 0.273 MJ/mole (65 Kcal/mole).[16] The viscosity at stress-relief annealing temperature is 10^{13} poises ($\sim 10^{8}$ lb-s/in.^{2}).[17] In our calculation, k is equal to 10^{14} poises ($\sim 10^{9}$ lb-s/in.^{2}) at temperature equal to half of the melting point. Viscosity values at other temperatures can be evaluated by Equation (21) with the preceeding information. Consequently, $\dot{\varepsilon}_0$ and, hence, $\dot{\varepsilon}$ can be calculated for various temperatures. Figure 7 shows the ductility dependence on strain-rate at various testing temperatures. Even though the shape of the curves remains the same, the ductility is very sensitive to temperature and strain-rate. It becomes evident that ductility loss is likely to occur within a small temperature range as temperature increases.

Figure 8 illustrates the ductility change for two x values and two strength ratios. It is shown that ductility can be improved by an order of magnitude, while x is increased by a factor of 2.5. A weaker improvement in ductility by increasing Ω is also demonstrated. Figure 8 also indicates that the ductility approaches a limit as $\dot{\varepsilon}$ decreases. Such limiting values as a function of x, as well as Ω, are shown in Figure 9. It appears that significant loss of ductility would only occur for x smaller than 0.01.

Ductility can actually be estimated from Equations (13) and (18) by assigning appropriate values to each parameter. If we take

Ω = 0.8

A' = 0.2

σ_o = 1034 MPA (150 ksi)

x = 0.001

μ = 0.07

k = 10^{14} poises ($\sim 10^9$ lb-s/in.^{2})

d = 0.051 mm (0.002 in.)

A = 0.1

σ = 552 MPa (80 ksi)

we have $\dot{e}/\dot{e}_g = 0.015$; and if ϵ_{gc} is 10%, the ductility is then 0.15%. Recognizing the uncertainties in the choice of parameters, the success of the model, in describing the experimentally observed features, provides confidence in its further development as a quantitative description of ductility loss.

CONCLUDING REMARKS

Based on Hart's model of intergranular failure, a mechanical model describing the tensile ductility loss at elevated temperatures for austenitic stainless steels and nickel base superalloys was derived. It was determined that the nature of failure is a highly localized ductile fracture mechanism. The model introduced two microstructure parameters, namely the fraction of the affected zone of the grain boundary to the grain size, x, and the strength ratio of the affected zone to the matrix of the grain, Ω. It is demonstrated that x is the dominant factor and that the ductility loss is not likely to occur when x is larger that 0.01.

The model developed here is qualitatively very successful in describing ductility trends in the intergranular failure regime. The success achieved suggests that detailed microstructural examinations of the grain boundary region be performed to provide data for more quantitative calculations. Further, generalization of the mechanical model to incorporate non-Newtonian grain boundary sliding and strain-hardening effects may be warranted.

REFERENCES

1. Fish, R. L. and Hunter, C. W., "Tensile Properties of Fast Reactor Irradiated Type 304 Stainless Steel," ASTM STP 611, pp. 119-138 (1976).

2. Raj, Rishi and Ashby, M. F., "Intergranular Fracture at Elevated Temperature," Acta Metallurgica, 23, pp. 653-666 (1975).

3. Waddington, J. S. and Lofthouse, K., "The Effects of Irradiation on the High Temperature Fracture of Stainless Steel," J. of Nuclear Materials, 22, pp. 205-213 (1967).

4. Williams, J. A., "A General Approach to Creep Fracture Resulting from Wedge Crack Growth," Phil. Mag., 20, pp. 635-639 (1969).

5. Gifkins, F. D., "A Mechanism for the Formation of Intergranular Cracks When Boundary Sliding Occurs," Acta Metallurgica, 4, p. 98 (1956).

6. McMahon, C. J., Jr., "Intergranular Fracture in Steels," Materials Science and Engineering, 25, pp. 233-239 (1976).

7. Hart, E. W., "Intergranular Failure," G. E. Technical Report, No. 69-C-334 (1969).

8. Rhines, F. N.; Bond, W. E.; and Kissel, M. A., "Grain Boundary Creep in Aluminum Bicrystals," Trans. of ASM, 48, pp. 919-951 (1956).

9. Sih, G. C., Editor, Methods of Analysis and Solution of Crack Problems, Noordhoff International Publishing, (1973).

10. Morris, D. G., "Creep in Type 316 Stainless Steel," Acta Metallurgica, 26, pp. 11413-1151 (1978).

11. Rice, J. R., "A Path Independent Integral and the Approximate Analysis of Strain Concentration by Notches and Cracks," Trans. ASME, Series E, J. Applied Mechanics, 35, pp. 379-386 (1968).

12. Wells, A. A., "Application of Fracture Mechanics at and Beyond General Yielding," British Welding Research Association, Research Report, M13/63 (1963).

13. Machlin, E. S., Discussion of "Mechanisms of Intergranular Fracture at Elevated Temperatures," by Gifkins, R. C., from Fracture, Edited by Averbach, B. L.; Felbeck, D. K.; Hahn, G. T.; and Thomas, D. A.; MIT Press (1959).

REFERENCES (Cont'd)

14. McLean, D. and Framer, M. H., "The Relation During Creep Between Grain Boundary Sliding, Subcrystal Size, and Extension," J. Inst. Metal, 85, pp. 41–50 (1956).

15. Garofalo, F., Fundamentals of Creep and Creep-Rupture in Metals, MacMillan Series in Materials Science, The MacMillan Co. (1965).

16. Cottrell, A. H., The Mechanical Properties of Matter, Chapter 7, Fluidity and Viscosity, John Wiley and Sons, Inc. (1964).

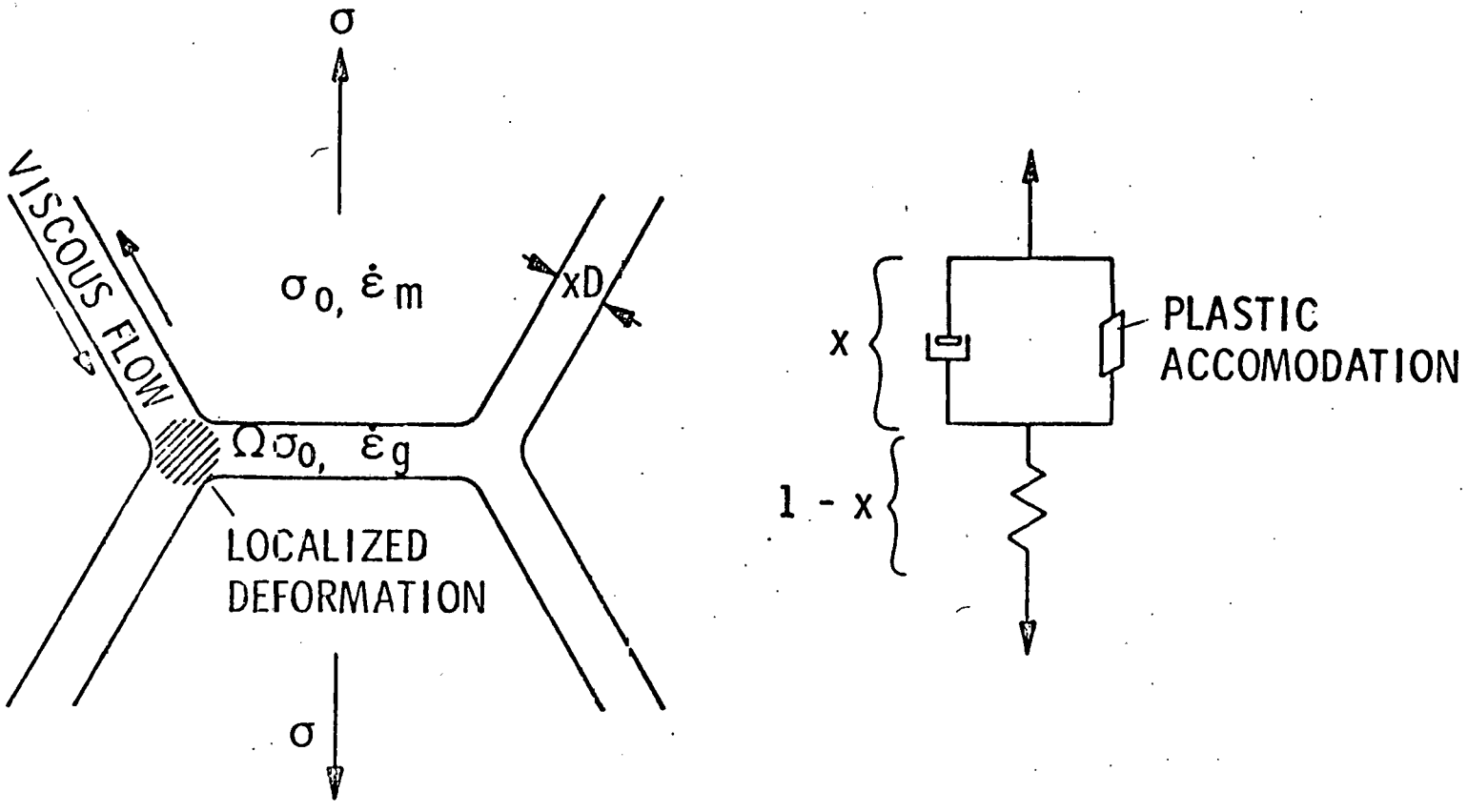

Fig. 1 Schematic and Rheological Diagrams of Proposed Model

HEDL 7810-110.2

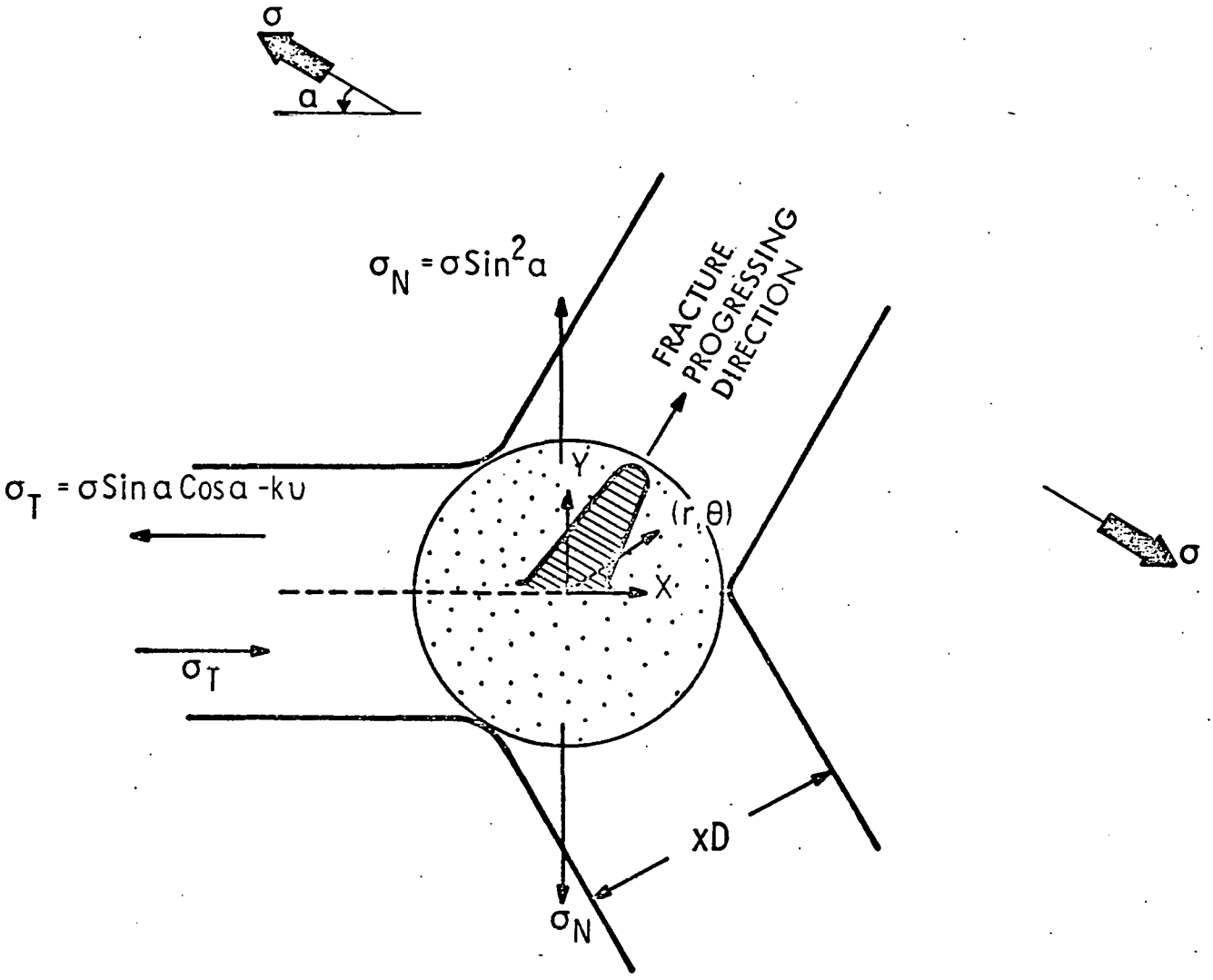

Fig. 2 Details Near the Triple Point

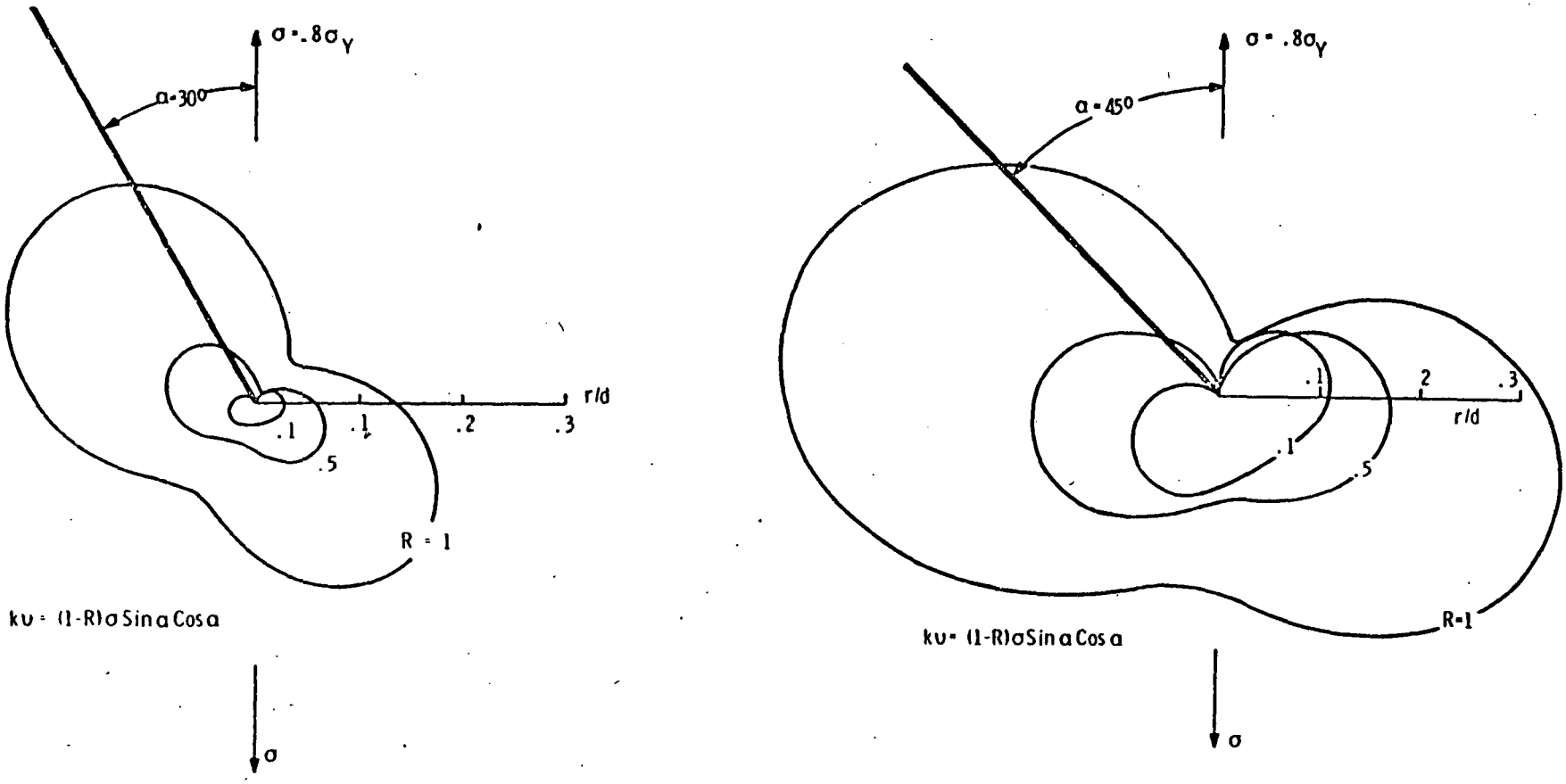

Fig. 3 Plastic Zone Ahead of an Inclined Crack Tip with Tangential Friction Force Along the Cracked Surface

HEDL 7810-110.7

HEDL 7810-110.6

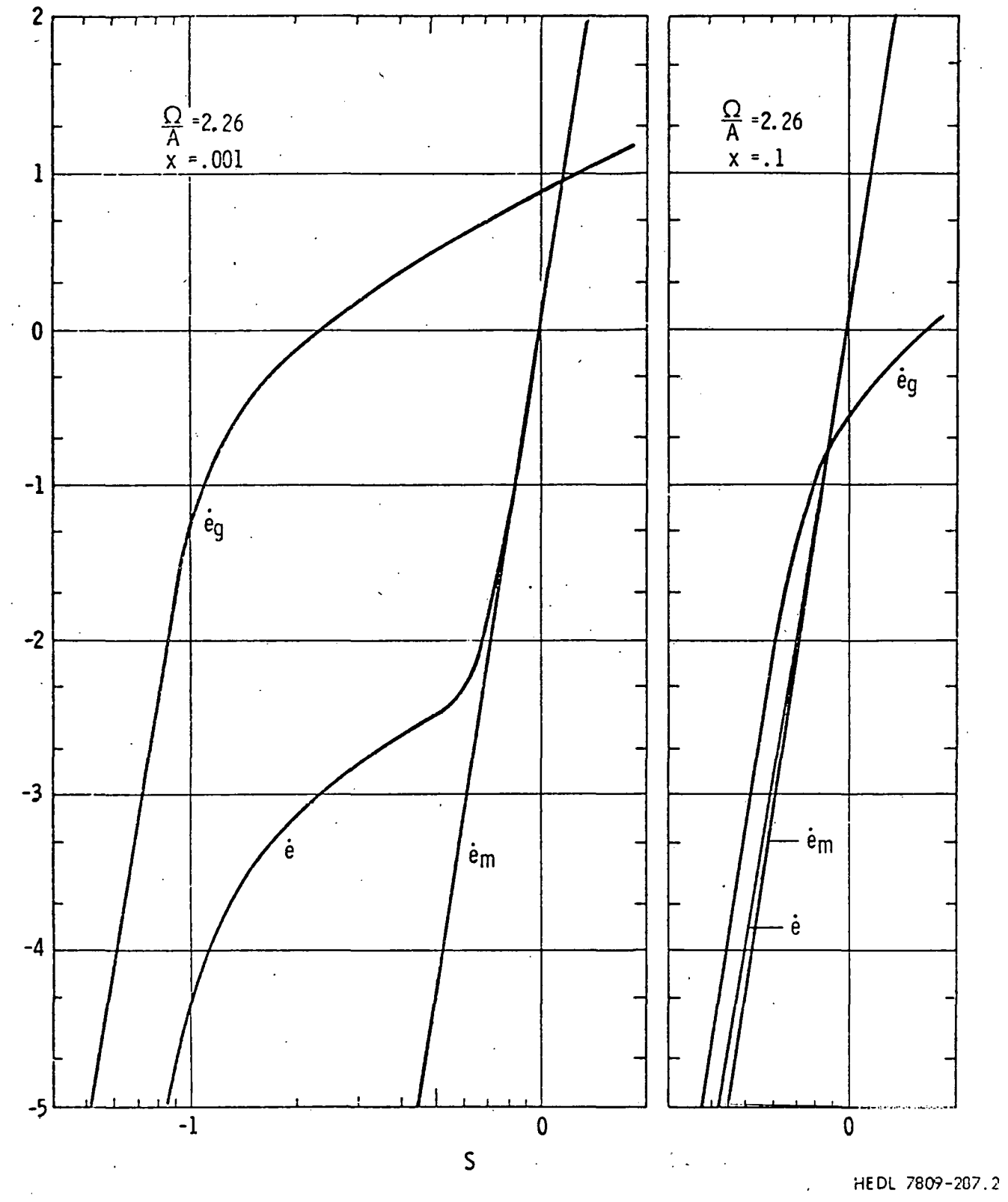

Fig. 4 Characteristic Strain and Strain-Rate Behaviors Predicted by the Model.

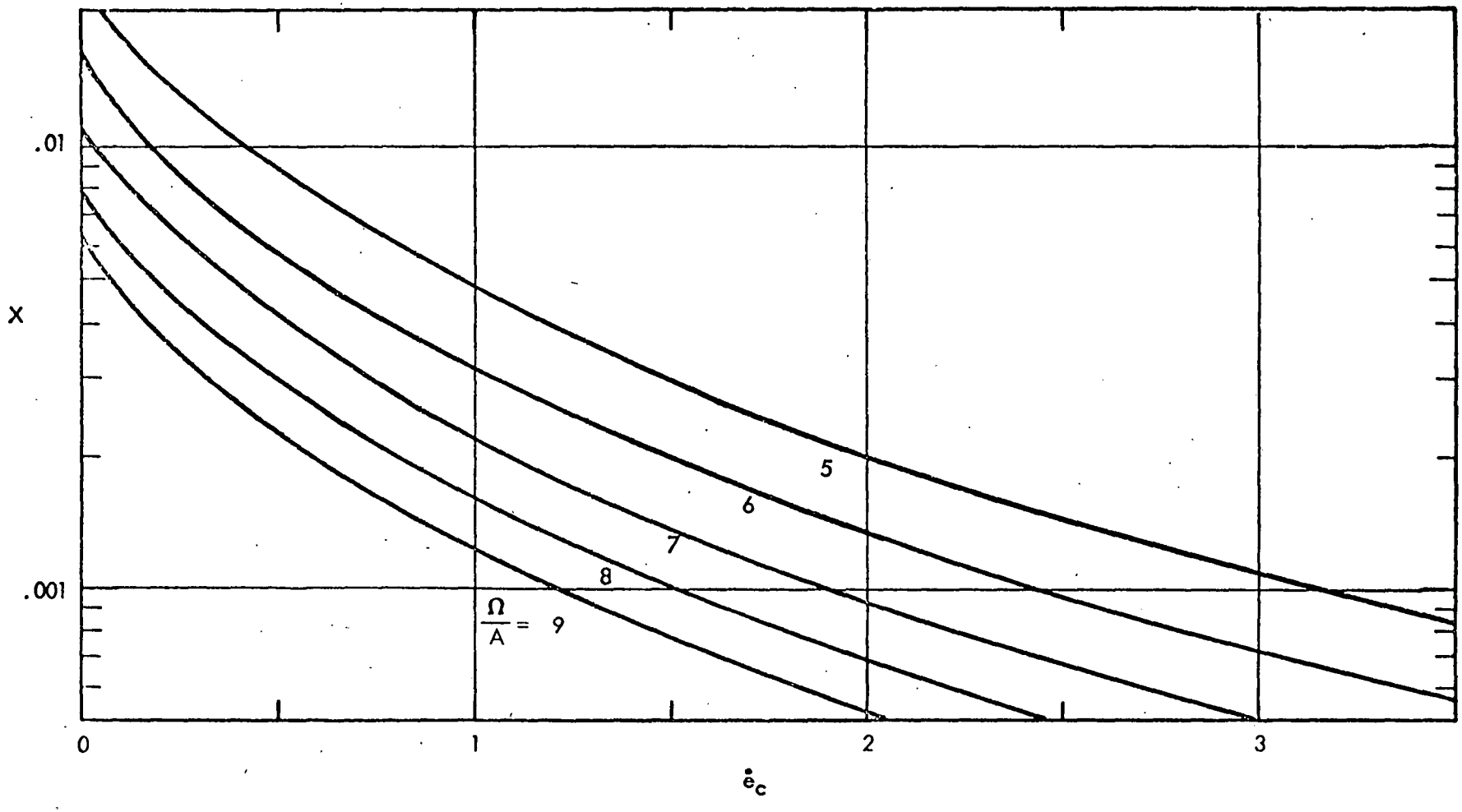

Fig. 5 Functional Dependence of Critical Strain-Rate Below which the Loss of Ductility Occurs with Respect to Microstructure Parameters x and Ω

HEDL 7811-027.1

MECHANICAL MODEL FOR DUCTILITY LOSS

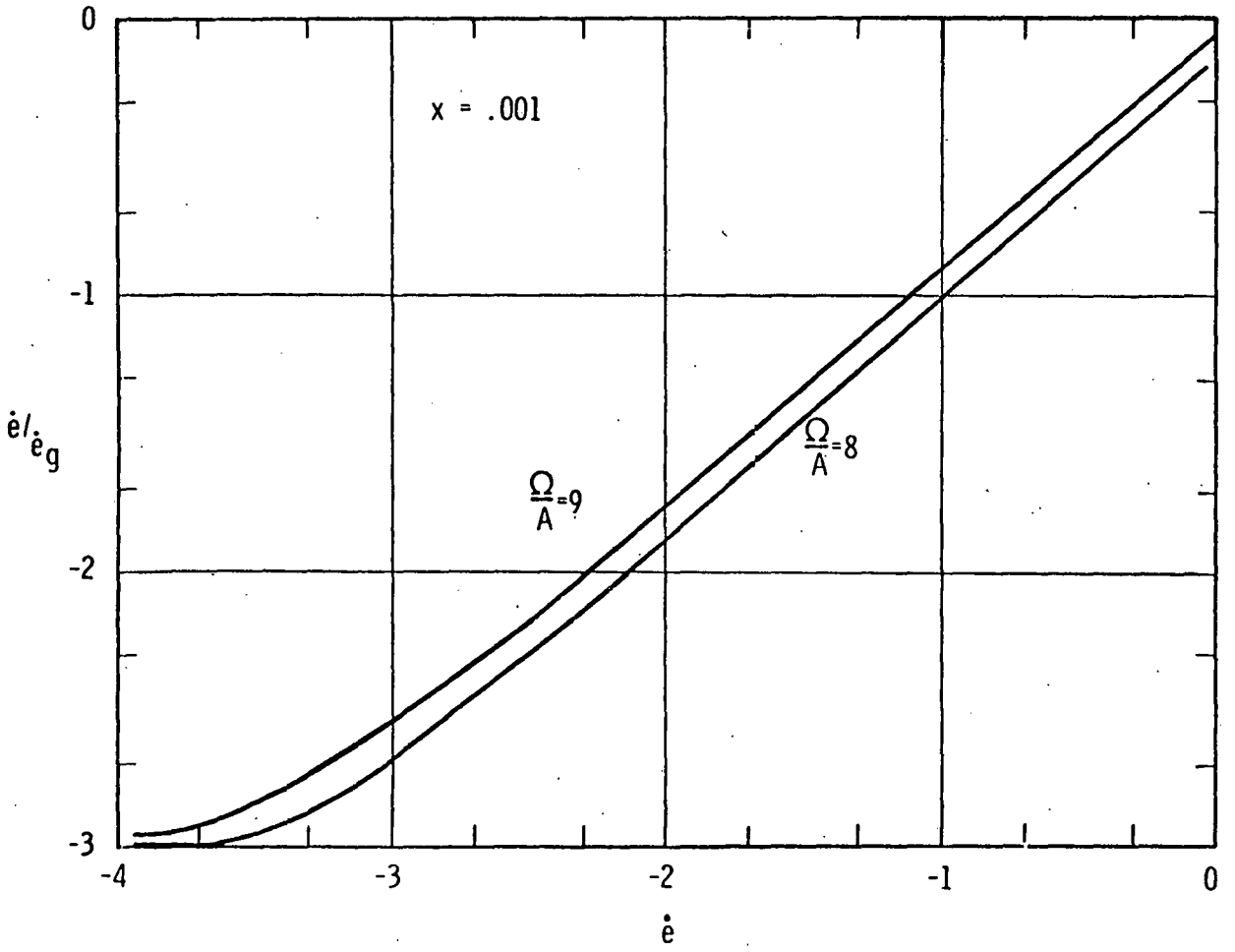

HEDL 7810-110.4

Fig. 6 Strain-Rate Sensitivity of Ductility Loss

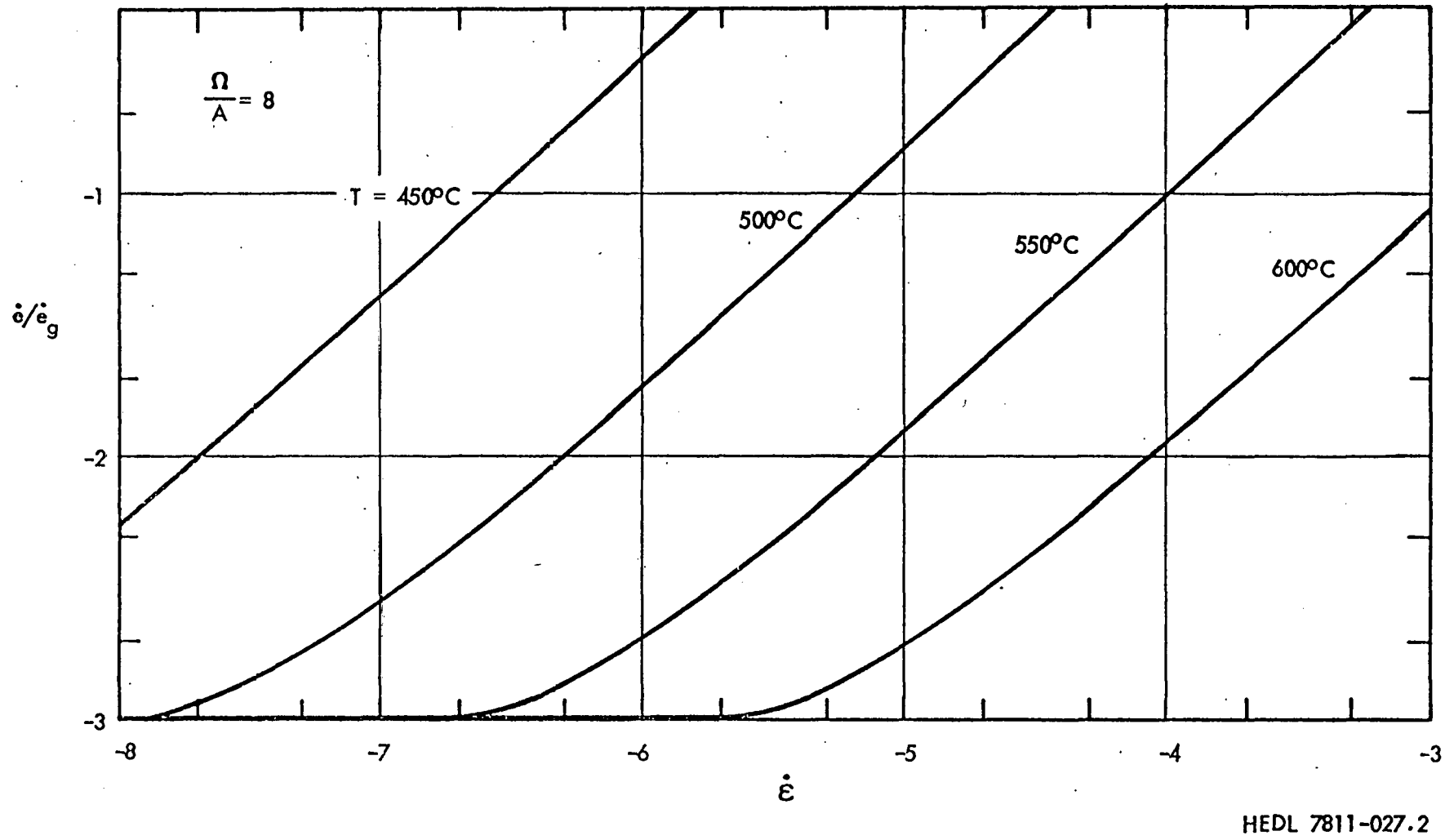

Fig. 7 Ductility as Function of Strain-Rate at Various Temperatures

MECHANICAL MODEL FOR DUCTILITY LOSS

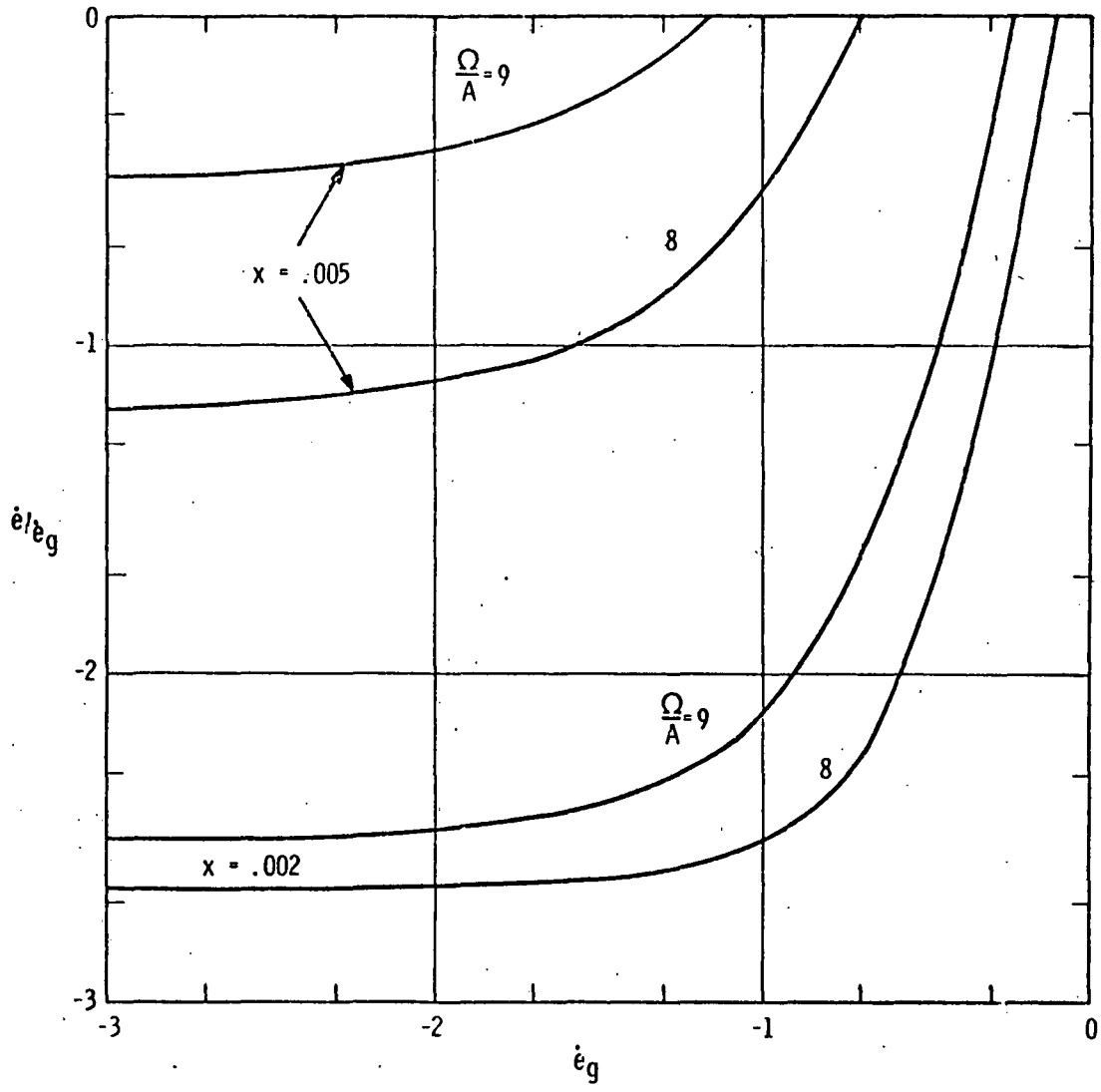

HEDL 7810-110.5

Fig. 3 The Effect of Microstructure Parameters on Ductility

MECHANICAL MODEL FOR DUCTILITY LOSS

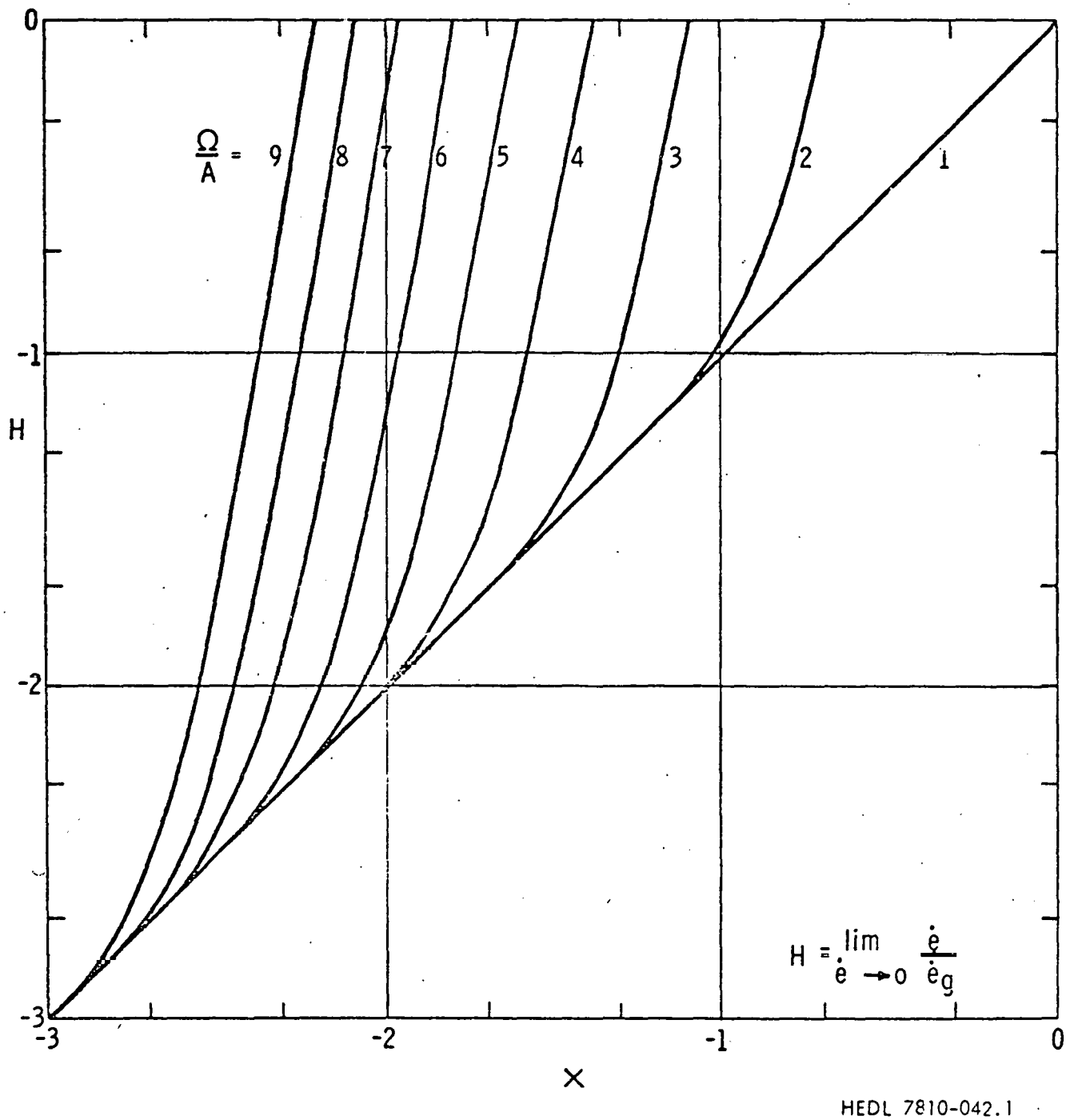

Fig. 9 Limiting Ductility When Strain-Rate Approaches Zero as a Function of x and Ω